DRAFT | Peer Review Purposes Only | Not for Citation

Estimating the Abundance of Outmigrant Juvenile Chinook Salmon from Rotary Screw Traps at Knights Landing and Tisdale Sites on the Sacramento River, California

Authors

Josh Korman, Ecometric Research; Liz Stebbins, FlowWest; Ashley Vizek, FlowWest; Erin Cain, FlowWest; Brett Harvey, California Department of Water Resources

Acknowledgments

The data used in this modeling effort are rich and extensive—in some cases, data collection has been ongoing since the late 1990s. This work would not have been possible without the field staff that collected daily rotary screw trap data over many years, and the data stewards who managed that data. We specifically acknowledge the current data collectors and stewards Anna Allison, Nicolas Bauer, Drew Huneycutt, Jeanine Phillips, and Corey Fernandez who assisted in this effort, curating and making compatible data used in analysis, and providing valuable insights that contribute to the modeling process.

We also thank the Spring-run Juvenile Production Estimate Core Team, Modeling Advisory Team, and Interagency Review Team for their useful comments and advice.

Work by Ecometric Research and FlowWest on this project was supported by the California Department of Water Resources.

Executive Summary

In 2024, the California Department of Fish and Wildlife issued an Incidental Take Permit (ITP) to the California Department of Water Resources (DWR) for operation of the State Water Project. As part of ITP Condition of Approval (COA) 7.9.3 DWR agreed to lead an interagency Core Team in the development of a modeling approach for calculating an annual Juvenile Production Estimate (JPE) for spring-run Chinook salmon (*Oncorhynchus tshawytscha*) (spring-run) produced in the Sacramento River watershed, and then use this approach to calculate a JPE annually beginning with the 2026/2027 migration season.

This chapter describes an important step toward that objective: the estimation, for all years having adequate historical data, of spring-run outmigrant abundance at rotary screw trap (RST) sites on the mainstem Sacramento River. These outmigrant abundance estimates, including quantification of the uncertainty of these estimates, will be used to fit (i.e., calibrate parameters of) multiple candidate JPE models. The abundance estimates and the dataset assembled to produce them will also be used to improve the structure and accuracy of other existing and future models guiding resource management in California's Central Valley, including a spring-run life cycle model as required under ITP COA 7.9.4, and the suite of salmon life cycle models produced by the interagency Science Integration Team, a technical group tasked with guiding restoration funding of the Central Valley Project Improvement Act. In addition, this chapter will aid the Core Team with an additional required task: reviewing data produced by spring-run monitoring programs in the mainstem Sacramento River, and recommending adjustments and augmentations to that monitoring to improve the ability of monitoring data to support calculating an annual JPE, and updates to the JPE and life cycle models.

An extensive network of RSTs is used to monitor the abundance of outmigrant juvenile Chinook salmon from streams and rivers in the Central Valley. To estimate the abundance of outmigrants over a trapping period each year, catches are expanded (divided) by the estimated proportion of fish that are captured when passing the RST. This proportion, commonly referred to as trap efficiency or capture probability, can be estimated from mark-recapture data. A variety of statistical modeling approaches can be used to convert catch and efficiency data into estimates of capture probability and abundance, but currently, there is no agreed-upon method for Central Valley RST data. This limits the utility of RST information. This chapter describes a new model that estimates abundance of juvenile Chinook outmigrant abundance at RST sites on the mainstem Sacramento River to support development of a spring-run JPE model. The model is similar in structure to the one applied to RST data from Sacramento River tributaries.

Central Valley RST programs use a two-sample mark-recapture approach to estimate abundance of outmigrant juvenile Chinook salmon. Fish are initially

captured (or taken from a hatchery), marked, and released during a first sample. A second sample is then taken from the population that consists now of both marked and unmarked fish. The number of marked and unmarked fish in the second sample is then used to estimate the abundance of fish that passed the RST location. The simplest approach to analyzing such data, the Peterson estimate, calculates abundance by dividing the total number of unmarked fish caught over the trapping season by the average capture probability of the RST as determined by efficiency trial data (i.e., release of marked fish and later recapture of a proportion of them). The Peterson estimate inherently assumes capture probability does not vary over the trapping season, as we might expect would occur due to changes in flow, water temperature, turbidity, or other factors. The stratified Peterson estimator calculates abundance over shorter time intervals (e.g., by week) and then sums the weekly estimates to generate an annual (trapping season) value. This approach avoids the assumption that capture probability is constant over time. However, it is a data-intensive approach because it requires catch and efficiency trial data (i.e., release of marked fish) for all weeks in a trapping season. For RSTs in the mainstem Sacramento River, there have been occasional weeks that were not sampled, and in some cases a very limited number of efficiency trials were conducted in a trapping season.

To address the challenges of data limitations in RST programs, Bonner and Schwarz (2011) developed the Bayesian Temporally Stratified Population Analysis System (BT-SPAS). This hierarchical Bayesian model (HBM) estimates capture probability for each stratum (e.g., week) in a trapping season based on the available efficiency trial data for that season. The approach provides a way to estimate capture probability when there are missing efficiency trial data for some weekly strata. BT-SPAS uses a spline method to estimate abundances, which improves precision of abundance estimates when there are missing efficiency trial data or where existing efficiency trial data are uninformative. The BT-SPAS spline approach does not assume abundance estimates are completely independent over time (e.g., weekly strata) like the stratified Peterson estimator does, so it can also estimate abundance in strata that are not sampled. BT-SPAS was originally developed for analyzing juvenile Chinook salmon RST data from the Trinity River (Schwarz et al. 2009, Som and Pinnix 2014), and has since been applied to rivers in the Central Valley and elsewhere (e.g., Pilger et al. 2019).

Data from Central Valley RST programs (including data from RSTs on the lower Sacramento River) have some unique limitations that preclude the use of BT-SPAS in most years. As previously mentioned, a limited number of efficiency trials are available for most years. Also, there may be sustained periods when RSTs were not fished, especially early or late in the trapping seasons. Thus, we developed a modified version of BT-SPAS called BT-SPAS-X, using “X” for extension, to address these limitations in Central Valley RST data. Chapter 4 describes a version of this model that was applied to RSTs located on Sacramento River tributaries.

This chapter describes a similar version of BT-SPAS-X that estimates abundance for Knights Landing and Tisdale RST sites on the mainstem Sacramento River. The main advancement of the BT-SPAS-X model is that, when estimating abundance for a particular year at an RST site, the model uses efficiency trial data from that year along with other years from that site to inform trap efficiency estimates for any given week. Owing to this approach, BT-SPAS-X provides more reliable estimates of capture probability and abundance in years when no or few efficiency trials are conducted.

In this chapter, we describe application of BT-SPAS-X to RST data from the Knights Landing and Tisdale RST sites on the Sacramento River. While the tributary version of BT-SPAS-X jointly estimates abundance for all tributary RST sites, which allows estimation of abundance in tributaries with few or no efficiency trial data, the mainstem version of the model estimates abundance separately for Knights Landing and Tisdale RST sites. The mainstem model is similar to the tributary model, but the mainstem model does not assume that capture probability parameters for each RST site arise from a common distribution across RST sites. The mainstem model assumes a common distribution only across years within each RST site.

The mean of observed capture probabilities at the Knights Landing (n=139) and Tisdale (n=47) RST sites were 0.47% and 0.25%, respectively. These capture probabilities are approximately 15-fold lower than estimated mean for Sacramento River tributaries of approximately 2.5%. The precision of capture probability estimates at mainstem RST sites was very low owing to the limited number of recaptures. Only 10% and 2% of the efficiency estimates at the Knights Landing and Tisdale RST sites had coefficient of variations (CVs) less than 0.25, respectively. In contrast, at least 50% of efficiency trials from 10 of 14 RST sites on tributaries of the Sacramento River had CVs of less than 0.25.

Predictions of capture probabilities at the Knights Landing and Tisdale RST sites fit the observed capture probabilities well (r^2=0.93 and 0.98, respectively). Estimated effects of discharge on capture probability were weak. There was considerable variability in modeled capture probability estimates around discharge-capture probability relationships, with process errors of 1.32 (standard deviation=0.11) and 1.11 (0.20) for Knights Landing and Tisdale RST sites, respectively. These estimates were approximately 2-fold larger and much more uncertain compared to the process error estimate for the tributary model (0.73 (0.03)). The greater unexplained variation in the mainstem model will lead to higher uncertainty in weekly abundance estimates in weeks without efficiency data compared to the tributary-based model.

Using the same set of years for both sites (2011 and 2014–2024), mean juvenile outmigration abundance (all run types) was approximately 12 million and 9.7 million at Knights Landing and Tisdale, respectively. Annual abundance estimates were highly correlated among these two RST sites across the overlapping

set of years (n=12, r^2=0.97). The average CV in annual abundance estimates (all run types combined) across years was approximately 30% at both RST sites. The range of CVs across years and sites was 18–51% at Knights Landing, and 19–46% at Tisdale. Generally, annual abundance estimates at mainstem RST sites were highly uncertain.

Annual outmigrant abundance estimates for spring-run were estimated by incorporating estimates of the weekly proportion of this run type from the probabilistic length-at-date (PLAD) model. Predictions indicate the proportion declined from values near 100% at the beginning of the run year to values less than 10% by approximately March. Annual estimates of outmigrant abundance for all run types were 4-fold higher at Knights Landing and 5-fold higher at Tisdale than the average of spring-run abundance estimates. Uncertainty in PLAD predictions led to higher uncertainty in annual estimates of abundance for spring-run outmigrants compared to outmigrants from all run types. For example, the average CV across years for all run types at Knights Landing was approximately 30%, compared to 42% for spring-run estimates. Minimum estimates of uncertainty across years were substantially lower for all run type abundance (i.e., 18–20%) estimates compared to spring-run estimates (29–32%).

The utility of Sacramento River mainstem abundance estimates for calculating a spring-run JPE may be low relative to tributary-based approaches owing to the large uncertainty in the estimates. It seems unlikely that the precision of mainstem abundance estimates can be improved by conducting more-frequent efficiency trials unless capture probabilities or the ability to estimate capture probabilities can be improved. Capture probability at mainstem RST sites is low, resulting in few recaptures even when a few thousand marked fish are released. Increasing the number of fish released by 3- or 4-fold would address this problem, but limitations in the availability of hatchery fish likely constrain this possibility. Conducting more efficiency trials within a year would have limited benefits for increasing precision of annual estimates if the resulting capture probability estimates are highly uncertain due to low numbers of recaptures. Alternate approaches to estimate capture probability at mainstem RST sites, such as paired coded-wire tag (CWT)/acoustic tag releases, could lead to improvements in the precision of abundance estimates. The U.S. Geological Survey recently demonstrated an example of such an approach for improving abundance estimates for the U.S. Fish and Wildlife Service Chipps Island Trawl; a similar application was less successful for the Sacramento River Trawl due to more riverine conditions causing lower baseline recapture rates. In addition, it is unclear whether this type of approach would provide representative capture probability estimates across the full size range of spring-run passing mainstem RSTs due to limitations on the size of fish that can be given an acoustic tag.

Contents

Tables

Figures

Appendices

Acronyms and Abbreviations

Term	Definition
CV	coefficient of variation
JPE	juvenile production estimate
spring-run	spring-run Chinook Salmon
LOOCV	leave-one-out cross validation
PLAD	probabilistic length-at-date

Term	Definition
Delta	Sacramento–San Joaquin River Delta
RST	rotary screw trap
BT-SPAS	Bayesian Temporally Stratified Population Analysis System
BUGS	Bayesian inference using Gibbs sampling
CWT	coded-wire tag
DAG	directed acyclic graph
DWR	California Department of Water Resources
HBM	hierarchical Bayesian model
ITP	Incidental Take Permit

1 Introduction

Rotary screw traps (RSTs) are commonly used in streams and rivers to monitor the abundance of outmigrating juvenile salmon and steelhead. An extensive network of RSTs is used to monitor the abundance of outmigrating juvenile Chinook salmon (*Oncorhynchus tshawytscha*) from streams in California's Central Valley. To estimate the abundance of outmigrants over a trapping period each year, catches are expanded (i.e., divided) by the estimated proportion of fish that are captured when passing the RST. This proportion, commonly referred to as trap efficiency or capture probability, can be estimated from efficiency trial data. Efficiency can be challenging to estimate and data to estimate it are frequently unavailable. A variety of statistical modeling approaches can be used to convert catch and efficiency estimates into abundance, but there is no agreed-upon method for estimating outmigrant abundance from Central Valley RST data, though efforts have been made (McDonald and Mitchell 2020). This limits the ability of RST data to evaluate outmigrant juvenile abundance across tributary and mainstem sites, which in turn limits the uses of RST information.

This chapter describes a model that was developed to estimate weekly and annual abundance of outmigrating spring-run Chinook salmon (spring-run) juveniles based on RST data from sites on the mainstem Sacramento River at the Knights Landing and Tisdale RST sites. The model was developed as part of a larger effort to devise alternative approaches for forecasting a juvenile production estimate (JPE) for spring-run from the Sacramento River and its tributaries. In Section 2, we begin by describing a new model that can estimate outmigrant abundance given data limitations that are common to many RST sites in the Central Valley, including those in the mainstem. This model estimates the weekly abundance of juvenile abundance from all run types of Chinook salmon. Estimates of weekly spring-run abundance are obtained by multiplying all run abundance by the proportion of the spring-run component each week, as determined by the probabilistic length-at-date (PLAD) model. In Section 3, we present results that highlight key aspects of model behavior and show how well predictions of capture probability and abundance fit the data. In Section 4, we end by summarizing the analysis main findings.

Annual and weekly outmigrant abundance estimates for mainstem sites on the Sacramento River provided by the model described in this chapter may become an important component of a larger spring-run JPE modeling effort. These abundance estimates could also be made available to researchers with other objectives such as life cycle modeling for spring-run and other runs of Sacramento River Chinook salmon.

2 BT-SPAS-X: A Modified Version of BT-SPAS to Address Data Limitations in Central Valley Rotary Screw Trap Data

This section describes how BT-SPAS-X can estimate outmigrant abundance given data limitations that are common to many RST sites in the Central Valley, including those in the mainstem.

We developed BT-SPAS-X, a modified version of BT-SPAS, to estimate the abundance of outmigrant juvenile Chinook salmon at RSTs in the mainstem Sacramento River and its tributaries (Figure 1). BT-SPAS-X addresses unique data limitations in Central Valley RST data. Like BT-SPAS, there are two major components of BT-SPAS-X: a hierarchical Bayesian model (HBM) is used to estimate capture probability for each weekly strata, and a Bayesian penalized spline model is used to estimate abundance given the catch of unmarked fish and estimates of capture probability.

Following estimation of weekly juvenile abundance for all run types of Chinook salmon, estimates of the weekly spring-run proportion are combined with estimates of all run abundance from BT-SPAS-X to calculate the weekly abundance of spring-run juveniles.

In the equations that follow, variables beginning with Greek letters represent estimated parameters, bolded Roman letters represent data, and Roman subscripts represent indices of the variables (e.g., model week “t”).

2.1 Capture Probability

2.1.1 Estimation

The capture probability component of BT-SPAS-X jointly estimates the capture probabilities for all years and weeks at the Knights Landing or Tisdale RST sites on the Sacramento River by fitting the model separately to all RST mark-recapture data (i.e., efficiency trials) from each site. Capture probability (p) at RST site ‘s’ in year ‘y’ on week ‘w’ is predicted by:

Equation 1a

$$logit(p_{s,y,w}) = \beta\_S_s + \beta\_Q_s \cdot \boldsymbol{Q}_{s,y,w} + \varepsilon_{s,y,w},$$

Equation 1b

$$\varepsilon_{s,y,w} \sim dnorm(0, \sigma_P)$$

Where:

logit indicates that capture probability is estimated in logit space,

β_S is the estimated intercept for site s,

β_Q is the estimated effect of flow on capture probability,

Q is the average standardized flow for year y and week w, and

ε is a random effect drawn from a normal distribution with standard deviation σ_p. σ_p represents the amount of variation in capture probability not explained by the β terms.

This is the unexplained variation that is commonly referred to as process error. The ε terms are random effects that account for limitations of model structure to explain the variance of the data. For example, effects of flow on capture probability may vary over years within RST sites owing to changes in morphology near the site or a change in RST position. The use of random effects also avoids negative bias in variance estimates resulting from pseudo-replication (Millar and Anderson 2004).

The parameter β_S is the capture probability (in logit space) at the average discharge level. Flow values ($\boldsymbol{Q}$) were centered and standardized by subtracting the mean flow at a site across all years and weeks included in the estimation, and then dividing by the standard deviation of all these weekly flow values. Thus, if flow for a week was equal to the average value across all years and weeks, the standardized value of Q is zero, and the average capture probability is determined only by β_S_s and the random effect (because the product of $\beta\_Q_s \cdot \boldsymbol{Q}$ would be zero). Note that because flow was standardized to mean flow *within* each RST site, rather than mean flow *across* all sites combined, the flow covariate effect modifies capture probability based on variation in flow *within* an RST site, and does not predict variation in capture probability across RST sites. Differences in capture probability across sites is solely determined by β_S_s.

Unlike the tributary version of BT-SPAS-X, the intercept (β_S) and flow effect (β_Q) terms of the capture probability for each RST site in the mainstem Sacramento River are assumed to be independent and therefore not drawn from common normal hyper-distributions. The number of mainstem RST sites (n=2) is too low to estimate the parameters of a common across-site distribution. Prior distribution for these parameters were uninformative zero-centered normal distributions:

Equation 2a

$$\beta\_S_s \sim dnorm(0,1000)$$

Equation 2b

$$\beta\_Q_s \sim dnorm(0,1000)$$

Where:

The first term represents the mean of the normal prior and the second its standard deviation

The capture probability model was fitted to the RST efficiency data using a binomial (dbin) data likelihood:

Equation 3

$$r_{s,y,w} \sim dbin(p_{s,y,w}, R_{s,y,w})$$

Where:

r is the observed number of marked fish that were recaptured, and

R is the number of marked fish that were released.

The terms of the capture probability model (Equations 1 and 2) were estimated by applying the model to all weekly observations of releases and recaptures at each mainstem RST site. Estimated site, year, and week deviates ($\varepsilon_{s,y,w}$) varied across observations to fit to the data (i.e., p values close to *r*/*R*). The deviates can be thought of as residuals that are approximately the difference between the observations of capture probability (*r*/*R*) and what was predicted by the β_S and β_Q effects in the capture probability model (Equation 1). In simple linear regression, the residuals are computed after the effects are calculated, and the residual variance is then calculated from these values. Because we used a hierarchical model, the deviates, called random effects, are jointly estimated along with variance of the normal distribution that generated them, as well as the other parameters in the model. The model maximizes the posterior probability by explaining much of the variation in capture probability observations based on β_S, and β_Q, and then picks up much of the remainder of the variation with the ε terms.

The data likelihood used to fit the capture probability model (Equation 3) accounts for differences in the amount of information across year and weekly strata within sites. Strata with a larger number of releases and especially a larger number of recaptures have more information about capture probability. As a result, the model fit relies more on these observations compared to those from strata with less information about capture probability (i.e., strata in which few recaptures were observed).

2.1.2 Applying BT-SPAS-X to Strata With No Efficiency Trial Data

The capture probability model in BT-SPAS-X can be used to predict capture probability in weeks when no efficiency trial data are available. For example, the model predicts capture probability using the appropriate site-specific estimates of β_S and β_Q, the value for Q for the year and week being estimated, and a random draw of an ε deviate from Equation 1b. If the unexplained process error for the capture probability model (σ_p) is high, the additional uncertainty associated with the random ε draw will be large. As a result, the uncertainty in capture probability for a week with no efficiency data will be higher compared to a week with efficiency data. In the latter case the ε deviate is much better defined and so capture probability is more certain.

The key difference between BT-SPAS and the mainstem Sacramento version of BT-SPAS-X with respect to capture probability is the latter jointly estimates capture probability for all weeks and years when trapping is conducted at an RST site. In contrast, BT-SPAS estimates weekly capture probabilities for each run year and site individually. By jointly fitting to all the mark-recapture data, BT-SPAS-X makes more reliable predictions of capture probability for run years where there are only a limited number of efficiency trials. Within an RST site, the model essentially borrows information from all run years and weeks where efficiency trials were conducted to estimate the capture probability for each particular run year and week. However, if there are substantive differences in capture probability across years due to factors other than flow, model predictions in weeks without efficiency trial data could be biased in some cases. The structure of the capture probability model presented here (Equation 1) can be modified in the future by adding covariates to produce more reliable predictions.

2.2 Abundance

2.2.1 Spline Model

BT-SPAS-X estimates abundance for weekly strata using a Bayesian penalized spline model. This is the same approach as BT-SPAS, but with the addition of a covariate effect to explain some of the variation in abundance over weeks. The model predicting the log of unmarked abundance in model week *t* is:

Equation 4

$$\log(U_t) = \sum_{k=1}^{K+q} \gamma_k \cdot \boldsymbol{B}_{\mathbf{k(t)}} + \phi \cdot \boldsymbol{X}_{\mathbf{s,y,w}} + \nu_t \quad \mathrm{I}(, \mathrm{lgN\_max_t}),$$

Where:

q is the order of the polynomial (*q* = 3 for the cubic spline used in this application),

k defines the index for each knot,

K is the total number of knots (one knot per four strata), and

t is an index for the weekly strata for the RST site and year that the model is applied to.

B is a pre-computed basis function that defines the contribution of each spline parameter γ to the prediction of abundance for each weekly stratum. ϕ is an estimated effect that allows extra-spline variation in abundance to vary as a linear function of covariate value ***X*** (e.g., flow). ν_t is a deviate that allows random extra variation in abundance beyond what is predicted by spline and covariate effects, and will be described in more detail below. The log of unmarked abundance is estimated in units of 1,000 for numerical precision, and converted to unlogged units prior to use in the data likelihood (Equation 3). The I(, lgN_max$_t$) term limits predicted abundance to a value no greater than lgN_max$_t$. This constraint can be set to a very high value so it has no effect on predictions, or a lower value for specific strata to constrain unrealistically high values resulting from sparse data. Results presented in this chapter are based on lgN_max set to u_t/0.0005. This maximum assumes that weekly capture probability can be no lower than 0.05%.

The model predicting the log of abundance by weekly strata (Equation 4) is the same as in BT-SPAS except for the addition of the covariate effect ($\phi \cdot \boldsymbol{X}_{\mathbf{s,y,w}}$). The spline component of the prediction can be thought of as the intercept in a simpler linear model. But rather than being a constant, it can vary in a smooth way across weekly strata. The covariate effect allows the predicted weekly estimated log of abundances to vary in a structured way around the spline-predicted intercepts based on the covariate values. The covariate effect was added to test the hypotheses that occasional increases in flow can lead to an increase in outmigration abundance. If this is the case, we would expect to see a positive estimate for ϕ_{flow}. Note covariate values *X* could represent any flow metric that may be developed, such as the within-tributary standardized average weekly flow, or a derived variable, such as the difference in flow from the previous week. Another alternative is to make *X* an indicator variable, for example taking on values of 0 or 1 if the relative flow increase is less than or greater than a specified threshold, respectively.

We assume that the prior distributions of spline parameters γ vary according to a second order random walk:

Equation 5a

$$\gamma_{k+1} - \gamma_k = \gamma_k - \gamma_{k-1} + \delta_k \text{ for k=2:}K,$$

Equation 5b

$$\delta_k \sim dnorm(0, \sigma_U)$$

Equation 5c

$$\gamma_{k=1:2} \sim dflat()$$

Where:

- δ_k is a normally distributed random variable with mean 0 and standard deviation σ_U.

Put more simply, the difference in adjacent spline parameters from knot k to k+1 is assumed to be related to the difference between values k-1 and k. The extent of the difference depends on the magnitude of the random normal deviates δ_k. If the deviates are large, because σ_U is large, the spline parameters can vary substantially across knots, and the spline will be flexible. Conversely, if σ_U is small, then the deviates will be smaller and spline parameters will vary less, and the spline will be stiffer. The certainty in U_t and its variability across strata determine the magnitude of the σ_U estimate. Different priors for spline coefficients are needed for the first two values of k. BT-SPAS and the mainstem version of BT-SPAS-X use a flat prior for k=1 and 2. A flat prior predicts the same prior probabilities for all values of γ_1 and γ_2.

Patterns in outmigrant abundance over strata may follow a general shape that can be well approximated by a spline and perhaps even covariate effects such as flow. However, it is also possible that there are sudden increases or decreases in outmigrant abundance due to random factors not accounted for in the abundance equation. In these cases, the spline and covariate effects would not fit the estimates of U_t well. To account for this possibility, extra-spline deviates for each stratum, ν_t, are drawn from a normal distribution with estimated standard deviation σ_{Ue}:

Equation 6

$$\nu_t \sim dnorm(\mu_{Ut}, \sigma_{Ue})$$

Where:

- μ_{Ut} is the prediction from Equation 4 excluding ν_t values.

If there is strong evidence for considerable extra-spline variation based on the pattern of U_t values, the estimate of σ_{Ue} will be larger to allow ν_t values to be more variable across strata. Although σ_{Ue} is sometimes referred to by the term "extra-spline variation," this term is only accurate if the covariate effect in Equation 4 is not estimated. If a covariate effect is estimated, σ_{Ue} is more accurately defined as the "additional variation not explained by both the spline and covariate effects." However, for brevity we use the term "extra-spline variation" for both cases. Like BT-SPAS, BT-SPAS-X uses uninformative gamma priors for the inverse of spline and extra-spline variances:

Equation 7a

$$\sigma_U^{-2} \sim dgamma(1, 0.05)$$

Equation 7b

$$\sigma_{Ue}^{-2} \sim dgamma(1, 0.05)$$

Parameter values that predict abundance (Equation 4) are estimated by comparing the abundance estimates to the catch data given the estimates of capture probability using:

Equation 8

$$u_t \sim dbin(p_t, U_t)$$

Note that values of u_t are adjusted to account for differences in trapping effort prior to running the model. To do this, the average number of hours an RST is fished each week (effort) over the modeled period (e.g., October–June) is computed for all run years for the tributary being modeled. If more than one RST is fished, the sum of hours across both RSTs is used in computing the average. The adjusted weekly catch is calculated as the product of the observed weekly catch and the ratio of the weekly effort (hours fished over week) to the average effort.

Capture probabilities used in the abundance model (π_t) are estimated from:

Equation 9

$$logit(\pi_t) \sim dnorm(\boldsymbol{\mu}_{p_t}, \boldsymbol{\sigma}_{p_t})$$

Where:

μ and σ terms are the weekly mean and standard deviation of weekly capture probabilities in logit space estimated from the posterior distributions of logit-transformed capture probability estimates generated by the capture probability model (Equation 1a).

Note μ and σ are treated as data in the abundance model. We use the cut() function in the Bayesian inference using Gibbs sampling (BUGS) modeling software so that predictions of π are not influenced by the fitting of u (unmarked catch) in the abundance model.

2.2.2 Estimation of Spring-run Chinook Salmon Abundance

A PLAD model (Chapter 6) is used to convert weekly estimates of total Chinook salmon abundance (all run types) for any site and run year (refer to Section 4.2) into estimates of spring-run abundance (srU_t) using:

Equation 10

$$srU_t = U_t \cdot srP_t$$

Where:

srP_t is the PLAD-based estimate of the spring-run proportion in week t.

PLAD estimates of srP_t are fit to site-specific genetic data and the length frequency of the RST catch in each week. PLAD results are available for both the Knights Landing and Tisdale RST sites.

2.3 Estimation

BT-SPAS-X estimates the parameters that predict weekly abundance of Chinook salmon U_t for all weeks for a given RST site and run year. BT-SPAS-X is run in three parts (Figure 2). First, the capture probability component of the model is run. BT-SPAS-X estimates capture probability for all weekly efficiency trials from all RST sites and the hyper-parameters from which they are calculated. Second, the posterior distributions of these parameters are passed to an R script to calculate capture probability for each week of the site-run year being modeled. Finally, the means and standard deviations of weekly capture probabilities generated from the script (Equation 9) are read-in by the abundance component of BT-SPAS-X to estimate weekly and annual abundance. This approach ensures that the abundance component of BT-SPAS-X does not influence the parameters determining capture probability (hence the red triangle in Figure 2). Thus, capture probability parameters that determine weekly values for any run year (within an RST site) will be the same for all run years.

Posterior distributions of the capture probability model were estimated using the stan statistical software (v 3.35.0; Stan Development Team 2024) called from the rstan library (v 2.35.0) from R (v 4.4.1; R Core Team 2024). Posterior distributions were based on 10,000 simulations per chain. Convergence was evaluated based on Gelman and Rubin's (1992) scale reduction factor. Weekly and annual abundances were estimated using the BUGS software (Spiegelhalter et al. 1999) called from the

R2WinBUGS (Sturtz et al. 2005) library. BUGS was used because it contains a cut() function that does not allow estimates of abundance to influence weekly capture probability values. Posterior distributions were based on taking every second sample from each of three chains from a total of 2,000 simulations per chain, after excluding the first 500 burn-in samples to remove the effects of initial values. These sampling characteristics were sufficient to achieve adequate model convergence as evaluated using the Gleman and Rubin scale reduction factor.

3 Application of BT-SPAS-X to Estimate Capture Probability and Outmigrant Abundance at Knights Landing and Tisdale Sacramento River Rotary Screw Trap Sites

This section describes BT-SPAS-X predictions of capture probability and outmigrant abundance for Knights Landing and Tisdale RST sites on the lower Sacramento.

3.1 Data Used in Modeling

We modeled an outmigration period of November 4 through May 27 (31 weeks) for the Knights Landing (27 years) and Tisdale (13 years) RST sites (Table 1). The mean of observed capture probabilities at the Knights Landing (n=139) and Tisdale (n=47) RST sites were 0.47% and 0.25%, respectively. These capture probabilities are approximately 15-fold lower than the average of estimated mean for Sacramento River tributaries of approximately 2.5% (Chapter 4). The precision of capture probability estimates was very low owing to the limited number of recaptures (Figure 3). Only 10% and 2% of the efficiency estimates at Knights Landing and Tisdale had CVs less than 0.25, respectively. In contrast, at least 50% of efficiency trials from 10 of 14 RST sites on tributaries of the Sacramento River had CVs of less than 0.25.

Mainstem Sacramento River RST data were not adequate to evaluate the effect of fish size at release on capture probability. Size at release was not recorded at the Tisdale RST site, and was only recorded for 23 of 139 trials at the Knights Landing RST site. Only six of these 23 trials had one or more recapture (r=1, 1, 7, 2, 2, 4); thus, estimates of capture probability for the few trials with size at release recorded were highly uncertain.

3.2 Capture Probability Model Results

Predictions of 139 and 47 capture probabilities at the Knights Landing and Tisdale RST sites (Equation 1) fit the observed capture probabilities (r/R, Table 2) well (r^2=0.93 and 0.98, respectively). The good fit occurred because the capture probability model estimates random-effect deviates for each efficiency trial. There was very weak statistical support for a flow effect on capture probability (Table 3). The slope of the flow effects was small and highly uncertain, especially at the Tisdale RST site (note higher CV of 0.64 and 95% credible intervals spanning zero).

There was considerable statistical shrinkage in the trial-specific estimates of capture probability, as seen by the difference between the expected values (r/R, blue open points in Figure 4) and the medians of the posterior distributions of the modeled

estimates (black solid points). When there was high sampling error in the modeled efficiency estimates due to few recaptures (as shown by the long vertical black lines in Figure 4), the model estimates shrunk toward the mean (the solid black line in Figure 4). In rare cases when capture probability of efficiency trials had higher precision as shown by narrower credible intervals, expected and modeled estimates were similar (i.e., less shrinkage).

There was considerable variability in modeled capture probability estimates (black points in Figure 4) around the discharge-capture probability relationship with process errors (σ_p in Equation 1b) of 1.32 (standard deviation=0.11) and 1.11 (sd=0.20) for the Knights Landing and Tisdale RST sites, respectively. These estimates were approximately 2-fold larger and much more uncertain compared to the process error estimate for tributary model (0.73, sd=0.03) (refer to Chapter 4). The greater unexplained variation in the mainstem model will lead to higher uncertainty in weekly abundance estimates in weeks without efficiency data compared to the tributary-based model.

3.3 Capture Probability and Abundance Estimates by Run Year

The following section examines model predictions of weekly capture probability and abundance for a single run year at the Knights Landing and Tisdale RST sites. We selected 2007 for Knights Landing and 2017 for Tisdale because there were five to six weeks with efficiency data at each site, which was close to the average for the years we modeled (6.2 years; Table 2). The intent in showing these results is to demonstrate critical aspects of model behavior. The full set of predictions for all years are available in Appendix A.

The juvenile (all run types) outmigration abundance estimate for the Knights Landing RST site in run year 2007 was 17.9 million fish with a CV of 21% (Figure 5a). The upper credible interval was high (25.2 million) because the model can estimate some very low capture probabilities, resulting in some very large estimates of weekly abundance. The extent of variation in capture probability estimates in a week was much higher in the majority of weeks that did not have efficiency trial data, which in turn led to very large uncertainty in weekly estimates of abundance. However, note that uncertainty in weekly capture probability and abundance was still high in weeks with efficiency data, owing to the typical very low number of recaptures. For example, in the week starting February 26, only three of 595 marked fish were recaptured, resulting in a 95% credible interval of capture probability of approximately 0.001–0.01 (i.e., 0.1% to 1%). This uncertainty is large in an absolute sense, but appears small relative to weeks without efficiency data. The estimated effect of discharge on capture probability was very limited (Figure 4, Table 3), resulting in small differences in the medians of weekly capture probability among weeks, even in cases when there were large differences in

discharge. The mean of estimated capture probability and abundance from the model agreed well with the Peterson estimates, indicating that model priors and constraints are not causing substantive bias. The juvenile abundance estimate for the Tisdale RST site in 2017 was 7.87 million fish, with a CV of 27% (Figure 5b). The upper limit on weekly abundance estimates (weekly catch/0.0005, the assumed lowest capture probability) can have a substantive influence on upper tail of the posterior distributions.

3.4 Time Series of Annual Abundance Estimates

Annual time series of juvenile outmigrant abundance at mainstem RST sites could be an important component of the spring-run JPE model (Figure 6). The across-year average of abundances (all run types combined) at these RST sites were approximately 16 million at Knights Landing and 9 million at Tisdale. However, these means are not directly comparable as the Knights Landing time series begins in 1996, and the Tisdale time series begins in 2011. Using the same set of years for both sites (2011 and 2014–2024), mean abundance was approximately 12 million at Knights Landing and 9.7 million at Tisdale. Annual abundance estimates were highly correlated among these two sites across the overlapping set of years (n=12, r^2=0.97). The average CV in annual abundance estimates (all run types combined) across years was approximately 30% at both RST sites (Table 4). The range of CVs across years and sites was 18–51% at Knights Landing, and 19–46% at Tisdale. In many years annual abundance estimates at mainstem sites were highly uncertain.

Annual outmigrant abundance estimates for spring-run were estimated by incorporating estimates of the proportion of this run type from the PLAD model. Predictions indicate the proportion declined from values near 100% at the beginning of the run year to values less than 10% by approximately March (Figure 7 and Appendix B). Annual estimates of outmigrant abundance for all run types was 4-fold higher at Knights Landing and 5-fold higher at Tisdale than the average of spring-run abundance estimates (Figure 8, Table 4). Uncertainty in PLAD predictions led to higher uncertainty in annual estimates of abundance for spring-run outmigrants compared to outmigrants from all run types (Table 4). For example, the average CV across years for all run types at the Knights Landing RST site was approximately 30%, compared to 42% for spring-run estimates. Minimum estimates of uncertainty across years (minimum CV in Table 4) were substantially lower for all run type abundance estimates (18–20%) compared to spring-run estimates (29–32%).

4 Conclusions

Annual estimates of spring-run juvenile outmigrant abundance are an essential component for the spring-run JPE approaches. Initial testing and evaluation of the mainstem version BT-SPAS-X to data from the Knights Landing and Tisdale RST sites on the lower Sacramento River indicates BT-SPAS-X is a suitable tool for translating catch and efficiency data into weekly and annual estimates of juvenile Chinook salmon outmigrant abundance (all run types and spring-run). However, owing to the limited number of recaptures of marked fish to estimate trap efficiency, weekly and annual abundance estimates at mainstem sites were highly uncertain.

It seems unlikely that the precision of mainstem abundance estimates can be improved by conducting more-frequent efficiency trials. Capture probability estimates from more than 180 weekly efficiency trials across the two mainstem RST sites was low, resulting in few recaptures even when a few thousand marked fish were released upstream of the traps. Increasing the number of fish released by 3- or 4-fold could address this problem assuming sufficient numbers of hatchery fish are available. Conducting more efficiency trials within a year would result in limited gains in precision in annual estimates of abundance as the resulting capture probability estimates will likely be highly uncertain due to low numbers of recaptures.

Alternate approaches to estimate capture probability at mainstem RST sites should be explored. For example, paired CWT/acoustic tagged releases of winter-run Chinook from hatcheries located upstream of the RSTs have been used to estimate capture probability at the Knights Landing and Tisdale RST sites (California Department of Fish and Wildlife, unpublished data). Estimates of capture probability from these experiments in 2014 and 2015 ranged from 0.03–0.69%, which are well within the range of the estimates provided in this chapter based on the traditional efficiency trial approach. The CWT/acoustic tagged approach would likely result in more certain estimates of capture probability than most of those presented in this chapter owing to the larger number of CWT recaptures at the RSTs (67–1,515, but uncertainty estimates were not reported for these studies). However, it is unclear how these estimates could be used to estimate abundance for the six-month or longer period each year over which capture probability and abundance must be estimated. The U.S. Geological Survey demonstrated an example of such an approach for improving abundance estimates for the U.S. Fish and Wildlife Service Chipps Island Trawl; a similar application was less successful for the Sacramento River Trawl due to more riverine conditions causing lower baseline recapture rates.

Uncertainty in weekly and annual abundance estimates reported here were sometimes strongly influenced by the assumption that capture probability could be no lower than 0.05%. This assumption will result in an underestimate of the upper

credible intervals of weekly abundance estimates. CWT/acoustic tag-based estimates could be used to define a more informative prior distribution of capture probability in BT-SPAS-X. For example, the lowest estimate of capture probability from these studies (0.03%) could be used to provide a minimum value for all weekly strata in BT-SPAS-X mainstem model runs. Capture probability estimates for larger outmigrants that can be acoustically tagged may not be representative of capture probabilities for the full size range of juvenile Chinook migrating past mainstem RST sites.

5 References

Bonner, SJ, and CJ Schwarz. 2011. "Smoothing population size estimates for time-stratified mark-recapture experiments using Bayesian P-Splines." *Biometrics* 67:1498–1507. https://academic.oup.com/biometrics/article/67/4/1498/7381210

California Department of Fish and Wildlife. n.d. Unpublished data placeholder

Gelman, A, and DB Rubin. 1992. "Inference from iterative simulation using multiple 651 sequences." *Statistical Science* 7:457–511. https://projecteuclid.org/journals/statistical-science/volume-7/issue-4/Inference-from-Iterative-Simulation-Using-Multiple-Sequences/10.1214/ss/1177011136.full

McDonald, T., and J. Mitchell. 2020. *CAMPR Analysis Documentation: Methods Embedded in the CAMPR Platform for Juvenile Salmonid Passage Estimation from Rotary Screw Trap Data*. Filename CAMPRdoc, last revision June 11, 2020.

Millar, RB, and MJ Anderson. 2004. "Remedies for pseudoreplication." Fisheries Research 70:387–407. https://www.sciencedirect.com/science/article/abs/pii/S016578360400181X

Pilger, TJ, ML Peterson, D Lee, A Fuller, and D Demko. 2019. "Evaluation of Long-Term Mark-Recapture Data for Estimating Abundance of Juvenile Fall-Run Chinook Salmon on the Stanislaus River from 1996 to 2017." *San Francisco Estuary and Watershed Science* 17(4). https://escholarship.org/uc/item/2z38p12t

Schwarz, CJ, D Pickard, K Marine and SJ Bonner. 2009. *Juvenile Salmonid Outmigrant Monitoring Evaluation, Phase II—December 2009*. Final Technical Memorandum for the Trinity River Restoration Program, Weaverville, CA. https://www.trrp.net/library/document/?id=369

Som, Nicholas A., and William D. Pinnix. 2014. *Evaluation of Reductions in Sampling and Mark–Recapture Effort on the Bias and Precision of Juvenile Chinook Salmon Outmigrant Estimates on the Trinity River, California*. Arcata Fisheries Technical Report TR 2014-20. Prepared for the U.S. Fish and Wildlife Service. https://www.researchgate.net/publication/280923594_Evaluation_of_Reductions_in_Sampling_and_Mark-Recapture_Effort_on_the_Bias_and_Precision_of_Juvenile_Chinook_Salmon_Outmigrant_Estimates_on_the_Trinity_River_California

Spiegelhalter, DJ, A Thomas, NG Best, and D Lunn. 2003. *WinBUGS User Manual*. Version 1.4. MRC Biostatistics Unit, Institute of Public Health, Cambridge, UK. https://legacy.voteview.com/pdf/WINBUGSmanual_2.pdf

Stan Development Team. 2024. *Stan Users Guide*. Version 2.35. https://mc-stan.org.

Sturtz, S, U Legges, and A Gelman. 2005. “R2WinBGS: A Package for Running WinBUGS from R.” *Journal of Statistical Software* 3:1–16. https://www.jstatsoft.org/article/view/v012i03

Tables and Figures

Tables

Table 1. Weeks of Sampling by Run Year at Knights Landing and Tisdale

Number of weeks of sampling by run year at Knights Landing and Tisdale rotary screw trap sites (RSTs) between November 4 and May 27. Run year 't' includes weeks from November 4 through December in calendar year 't-1' and January through May 27 in calendar year 't.'

Run Year	Knights Landing (weeks)	Tisdale (weeks)
1996	31	-
1997	31	-
1998	31	-
1999	31	-
2000	31	-
2001	31	-
2002	-	-
2003	31	-
2004	31	-
2005	31	-
2006	31	-
2007	31	-
2008	31	-
2009	31	-
2010	31	-
2011	31	31
2012	31	-
2013	-	31
2014	31	31
2015	31	31
2016	31	31
2017	31	31
2018	31	31
2019	31	31
2020	31	31
2021	31	31
2022	31	31
2023	31	31
2024	31	31
Total	27	13

Table 2. Total Releases and Recaptures, and Expected Efficiency Estimates

Total releases (R) and recaptures (r) and expected efficiency estimates (100*r/R) for juvenile Chinook salmon based on RST efficiency trials (aggregated to week) at Knights Landing (3.2a) and Tisdale (3.2b) RST sites on the Sacramento River.

Table 2a. Knights Landing

(n=139, average efficiency=0.47%)

Run Year	Julian Week	Releases	Recaptures	Efficiency (%)
1996	4	461	1	0.22
1996	5	1,012	28	2.77
1996	6	780	1	0.13
1996	7	1,153	1	0.09
1996	8	261	1	0.38
1998	2	5,197	44	0.85
1998	3	1,854	17	0.92
1998	4	2,356	3	0.13
1998	5	1,739	20	1.15
1998	6	1,797	10	0.56
1998	7	1,358	4	0.29
1998	8	861	2	0.23
1998	9	1,557	13	0.83
1998	10	916	10	1.09
1998	11	682	7	1.03
1998	12	5,327	138	2.59
1998	13	1,618	11	0.68
1998	14	311	1	0.32
1998	15	227	1	0.44
1998	16	295	0	0
1998	17	279	1	0.36
1998	18	337	1	0.3
1998	19	116	2	1.72
1998	20	54	0	0
1998	21	100	0	0
1998	24	218	0	0
1998	52	49	2	4.08
1999	51	111	0	0
1999	52	126	0	0
2000	5	1,417	6	0.42

Run Year	Julian Week	Releases	Recaptures	Efficiency (%)
2000	6	2,291	4	0.17
2000	7	6,111	160	2.62
2000	8	1,746	30	1.72
2000	9	769	6	0.78
2000	10	590	4	0.68
2000	11	171	0	0
2000	12	67	0	0
2000	13	80	0	0
2000	14	127	0	0
2000	16	181	0	0
2000	17	78	3	3.85
2001	5	393	2	0.51
2001	6	1,145	1	0.09
2001	7	91	0	0
2001	8	2,546	17	0.67
2001	9	1,164	9	0.77
2001	10	630	5	0.79
2001	11	469	2	0.43
2001	13	127	0	0
2001	17	843	0	0.57
2001	18	525	3	0.05
2001	19	4,428	2	0.5
2001	20	796	4	0.41
2007	7	3,701	15	0.1
2007	8	1,052	1	0.5
2007	9	596	3	0
2007	18	712	0	0
2007	51	341	0	0.08
2007	53	1,307	1	0
2008	1	3,500	0	1.01
2008	2	892	9	0.37
2008	5	9,792	36	0.36
2008	6	554	2	2.06
2008	7	243	5	1.43
2008	9	1,684	24	0
2009	5	250	0	0.77
2009	8	2,212	17	0.33
2009	9	2,761	9	0.18

Run Year	Julian Week	Releases	Recaptures	Efficiency (%)
2009	10	1,106	2	0
2009	11	1,106	0	0.65
2009	12	1,234	8	0.22
2010	3	465	1	0.09
2010	4	3,273	3	0.82
2010	5	1,096	9	0.25
2010	6	399	1	1.75
2010	9	171	3	0.42
2011	1	708	3	0
2011	8	370	0	0.24
2011	12	414	1	1.95
2011	13	205	4	1.47
2011	17	136	2	0.57
2012	4	2,291	13	1.53
2012	5	196	3	0.14
2012	12	696	1	1.44
2012	13	1,944	28	0
2012	16	284	0	1.05
2014	8	285	3	1.3
2014	10	1,078	14	0
2014	12	81	0	0
2015	6	2,870	0	2.35
2015	7	1,278	30	0
2015	12	570	0	0
2015	13	513	0	0
2016	2	3,202	43	1.34
2016	4	2,864	5	0.17
2016	6	632	0	0
2016	7	479	0	0
2016	8	489	0	0
2016	11	490	1	0.2
2016	12	488	0	0
2016	13	470	0	0
2016	14	516	7	1.36
2016	15	473	0	0
2016	16	419	1	0.24
2016	17	507	0	0
2016	38	334	1	0.3

Run Year	Julian Week	Releases	Recaptures	Efficiency (%)
2016	39	311	0	0
2016	41	304	0	0
2016	42	152	0	0
2017	3	1,407	2	0.14
2017	4	182	0	0
2017	10	987	1	0.1
2017	11	950	0	0
2017	12	906	2	0.22
2017	39	1,033	0	0
2017	42	1,311	1	0.08
2017	45	969	1	0.1
2017	48	1,126	2	0.18
2018	15	240	0	0
2018	43	1,105	0	0
2018	45	959	0	0
2018	48	947	1	0.11
2019	6	293	0	0
2019	11	1,114	0	0
2019	13	910	0	0
2019	15	1,913	0	0
2019	17	127	0	0
2019	45	642	0	0
2021	5	100	0	0
2021	6	401	0	0
2021	12	556	1	0.18
2021	13	128	0	0
2022	2	320	0	0
2022	10	500	0	0
2022	51	275	2	0.73
2022	52	212	1	0.47
2023	2	721	0	0
2023	15	1,217	4	0.33
2024	13	1,163	0	0

Table 2b. Tisdale

(n=47, average efficiency=0.25%)

Run Year	Julian Week	Releases	Recaptures	Efficiency (%)
2015	12	557	1	0.18
2015	13	421	2	0.48
2016	3	681	6	0.88
2016	6	358	1	0.28
2016	7	457	1	0.22
2016	8	493	0	0
2016	11	486	0	0
2016	12	511	0	0
2016	13	502	0	0
2016	14	511	1	0.2
2016	15	638	4	0.63
2016	16	632	0	0
2016	17	390	1	0.26
2016	39	318	2	0.63
2016	41	170	0	0
2016	42	500	1	0.2
2017	8	935	2	0.21
2017	13	250	0	0
2017	14	1,290	1	0.08
2017	37	1,170	1	0.09
2017	41	1,024	1	0.1
2017	43	1,168	2	0.17
2017	46	1,078	4	0.37
2018	44	1,084	2	0.18
2018	44	1,084	2	0.18
2018	46	1,004	1	0.1
2019	10	1,040	1	0.1
2019	12	857	0	0
2019	14	1,187	0	0
2019	16	997	0	0
2021	6	494	3	0.61
2021	10	298	0	0
2021	12	392	0	0
2022	10	517	3	0.58
2022	11	502	0	0

Run Year	Julian Week	Releases	Recaptures	Efficiency (%)
2022	12	500	0	0
2022	13	500	1	0.2
2022	14	478	1	0.21
2023	4	500	1	0.2
2023	6	494	0	0
2023	15	1,093	2	0.18
2023	16	993	12	1.21
2023	17	1,025	18	1.76
2024	3	431	4	0.93
2024	4	322	0	0
2024	11	1,054	0	0
2024	12	1,273	0	0
2024	13	1,072	4	0.37

Table 3. Statistics of the Estimated Posterior Distributions of β_Q_s

Statistics of the estimated posterior distributions of β_Q_s, the effect of standardized discharge on capture probability, at Knights Landing and Tisdale RST sites. Statistics include the mean, coefficient of variation (CV) and the lower and upper bounds of the 95% credible interval.

			Credible	Interval
Site	**Mean**	**CV**	0.025	0.975
Knights Landing	0.47	0.29	0.29	0.75
Tisdale	-0.35	0.64	-0.83	0.07

Table 4. Annual Abundance Estimates and Coefficient of Variation by Run Year

Annual abundance estimates and coefficient of variation in abundance estimates (as CV) for outmigrating juvenile Chinook salmon (all run types and spring-run only) by run year from November 4 to May 27 at Knights Landing and Tisdale RST trap sites. Also shown are the number of efficiency trials conducted each year.

Table 4a. Knights Landing

Run Year	All Run Efficiency Trials	All Run Abundance (thousands)	All Run CV%	Spring-run Abundance (thousands)	Spring-run CV%
1996	5	136	36%	30	47%
1997	0	26,729	21%	4,724	29%
1998	22	14,208	18%	3,011	26%
1999	2	17,486	26%	3,196	32%

Run Year	All Run Efficiency Trials	All Run Abundance (thousands)	All Run CV%	Spring-run Abundance (thousands)	Spring-run CV%
2000	12	3,870	27%	743	34%
2001	12	30,248	22%	5,278	33%
2002	-	-	-	-	-
2003	0	21,654	34%	TBD	TBD
2004	0	52,177	34%	TBD	TBD
2005	0	22,826	38%	TBD	TBD
2006	0	13,498	30%	TBD	TBD
2007	6	17,951	21%	4,380	33%
2008	6	17,928	21%	4,322	27%
2009	6	10,533	29%	1,571	31%
2010	5	19,740	35%	3,656	35%
2011	5	5,044	24%	1,117	33%
2012	5	6,694	27%	1,002	30%
2013	-	-	-	-	-
2014	3	85,312	51%	12,933	54%
2015	4	12,207	25%	2,832	31%
2016	16	10,676	39%	2,522	50%
2017	9	5,374	29%	1,361	37%
2018	4	911	41%	128	36%
2019	6	6,954	22%	1,171	29%
2020	0	4,557	37%	996	44%
2021	4	3,907	28%	590	32%
2022	4	2,587	32%	768	41%
2023	2	6,687	35%	1,813	44%
2024	1	6,195	34%	1,382	44%
Minimum	0	136	17.6%	30	26%
Average	5.1	15,781	30.1%	2,588	36%
Maximum	22	85,312	51.2%	12,933	54%

Table 4b. Tisdale

Run Year	All Run Efficiency Trials	All Run Abundance (thousands)	All Run CV%	Spring-run Abundance (thousands)	Spring-run CV%
2011	0	11,183	20%	2,362	28%
2012	-	-	-	-	-
2013	-	2,933	42%	849	44%
2014	0	55,244	45%	8,611	51%

Run Year	All Run Efficiency Trials	All Run Abundance (thousands)	All Run CV%	Spring-run Abundance (thousands)	Spring-run CV%
2015	2	7,233	45%	2,013	42%
2016	14	8,510	27%	1,936	36%
2017	7	5,079	23%	885	27%
2018	2	252	27%	48	31%
2019	4	3,109	21%	503	29%
2020	0	5,415	46%	1,595	51%
2021	3	3,192	37%	558	46%
2022	5	4,103	34%	1,395	43%
2023	5	7,881	27%	2,014	35%
2024	5	5,707	25%	1,452	36%
Minimum	0	252	19.5%	48	27%
Average	3.9	9,219	32.2%	1,863	38%
Maximum	14	55,244	45.8%	8,611	51%

Figures

Figure 1. Map of the Sacramento River and Tributaries

Map of the Sacramento River and tributaries showing the location of RST sites considered for use in the spring-run juvenile production estimate (JPE) modeling.

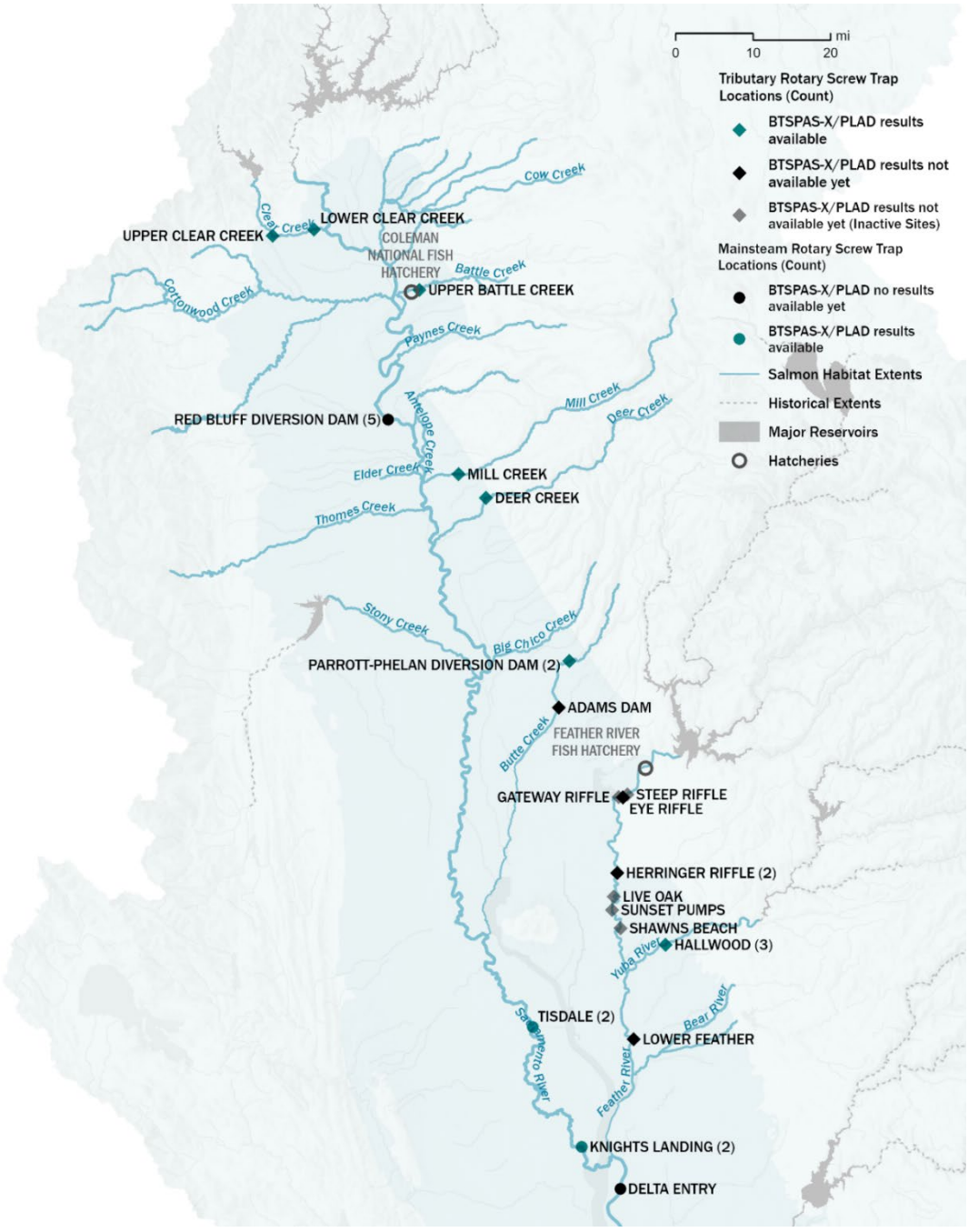

Figure 2. Directed Acyclic Graph Describing Relationship Among Estimated Parameters and Data

Directed acyclic graph (DAG) describing the relationship among estimated parameters (stochastic nodes denoted by Greek letters within ovals) and data (Roman bolded letters in squares) in the BT-SPAS-X mainstem model. Vertical position in the DAG denotes the parent-child relationship among nodes. The red triangle denotes that capture probability estimates influence abundance estimates but the converse does not occur. For simplicity, subscripts for site, year, and week are not shown.

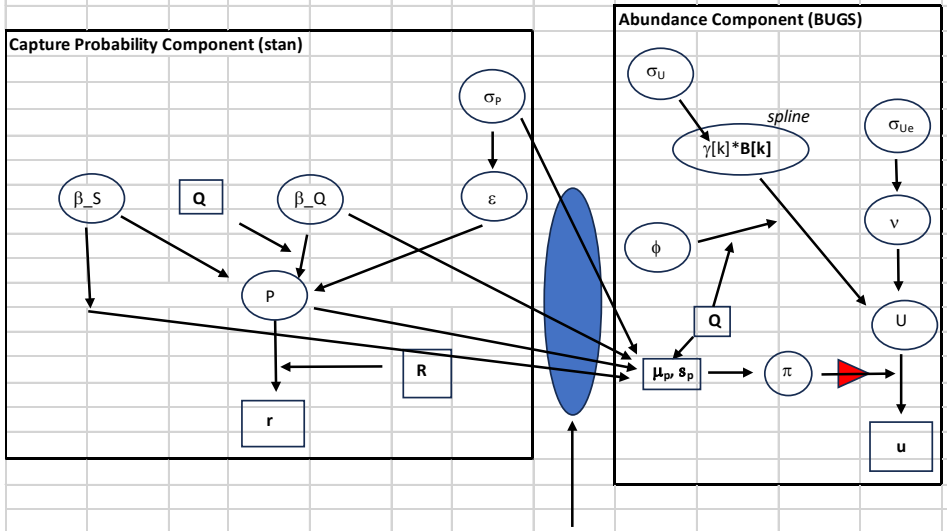

Capture Probability Model	
σ_Q	standard deviation of hyper-distribution for flow effect
σ_P	standard deviation of zero-centered normal distribution for unexplained error
β_S	site effect on capture probability for each site
β_Q	flow effect on capture probability for each site
P	Capture probability (trap efficiency)
ε	unexplained error in capture probability
r	observed recaptures
R	observed releases
Q	observed weekly average flow

Abundance Model	
σ_U	standard deviation controlling flexibilti of spline weekly abundance curve
γ	spline coefficient for each spline knot k with basis function **B**
ϕ	parameter controlling effect of flow on predicted weekly abundance
σ_{Ue}	standard deviation controlling extent of non-spline variation in weekly abundance
ν	weekly deviate added to spline-predicted weekly abundance
U	predicted weekly abundance
u	observed weekly catch
Q	observed weekly average flow
B	Basis function of each spline node
$\boldsymbol{\mu_p}$	mean of weekly capture probability
$\boldsymbol{\sigma_p}$	standard deviation of weekly capture probabilty
π	weekly capture probability

square boxes and bolded variables are data or variables treated as data
ovals denote stochastic nodes (things that are estimated)
vertical position denotes parent-child relationships. E.g., the site-specific intercept beta_S is a child of the site-effect hyper distribution defined by mu_S and sd_S
for simplicity of diagram, subscripts for site, year, and week are not shown
red triangle denotes use of cut() function so abundance model cannot influence weekly means and standard deviations of capture probability
cut() function removed from stan version of model

Figure 3. Capture Probability for Juvenile Chinook Salmon from Mainstem Sacramento River sites

Capture probability (trap efficiency) for juvenile Chinook salmon from mainstem Sacramento River sites. Red lines are contours showing how the precision of capture probability estimates varies as a function of the number of marks released and the capture probability. Contour values represent the CV of capture probability estimates, calculated from $CV = \sqrt{\frac{1-p}{R \cdot p}}$, where R is the number of releases and p is the capture probability (releases/recaptures). The title of each plot shows the total number of efficiency trials (aggregated to week) conducted at Knights Landing (top) and Tisdale (bottom) RST sites. The horizontal black line shows average of all capture probability values.

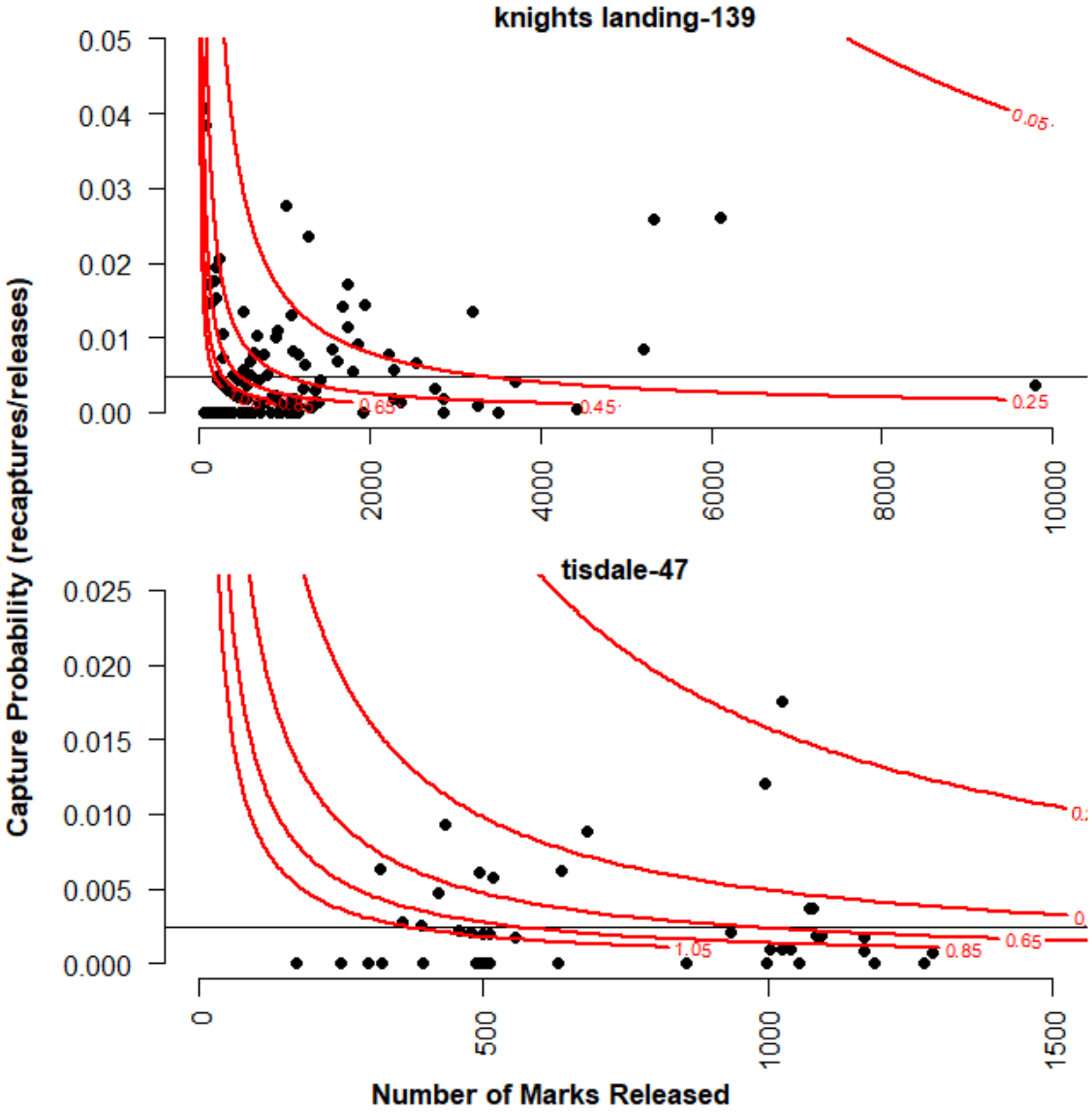

Figure 4. Relationship Between Standardized Discharge and Rotary Screw Trap Efficiency for Knights Landing (upper) and Tisdale (lower) Sites

Relationship between standardized discharge and RST efficiency for juvenile Chinook salmon at Knights Landing (top) and Tisdale (bottom) RST sites. Open blue points show the expected efficiency for each trial (recaptures/releases aggregated to week). Black points and vertical lines show the median predicted weekly efficiency estimates and 95% credible intervals from the model. The horizontal black line and dark grey shaded area show the median and 95% credible intervals for the predicted discharge-efficiency relationship. The light grey shaded area shows the 95% credible intervals that include effects of uncertainty in the discharge relationship and process error.

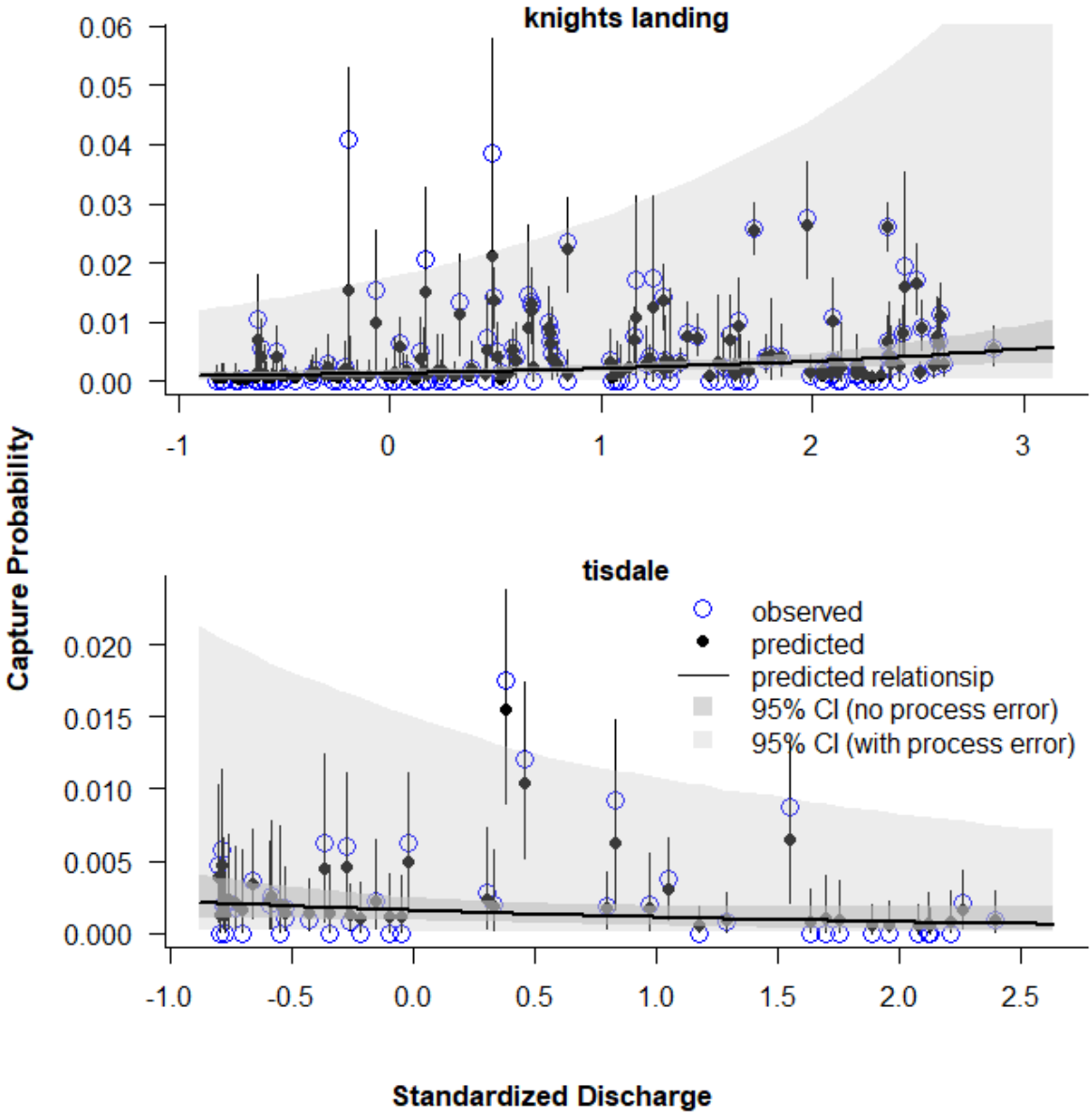

Figure 5. Predicted Abundance (upper) and Capture Probability (lower), Knights Landing and Tisdale Rotary Screw Trap Sites

Predicted abundance of juvenile outmigrant Chinook salmon (all run types and fry and smolt life stages combined, top panel) and capture probability (bottom panel) by weekly strata for select RSTs sites and run years. The height of the bars and black error bars show the medians and 95% credible intervals predicted by BT-SPAS-X. Bars in the top panels with dots above them and no open circles or numbers above them identify strata with no sampling data; bars in the bottom panel identify strata with no mark-recapture data. Numbers at the top of each plot show the unmarked catch (u, top panel), and the number of recaptures (r) and releases (R, bottom panel). Open circles show the Peterson estimates of abundance (U=u/p, error bars show 95% confidence intervals)) and capture probability (p=r/R). The line with points shows the average weekly discharge. The title shows the median total abundance estimate for the run year with 95% credible intervals in parentheses. The CV of the annual abundance estimate is also shown.

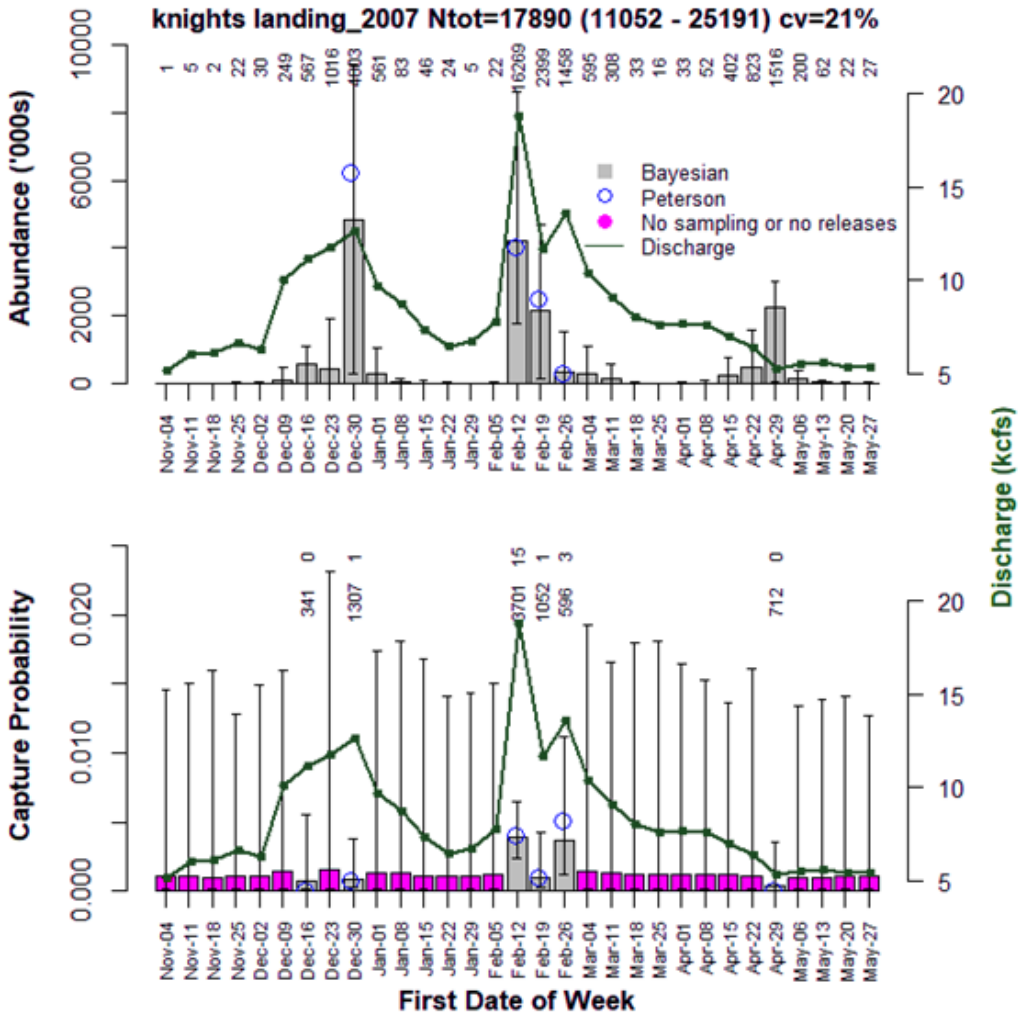

Figure 5, continued

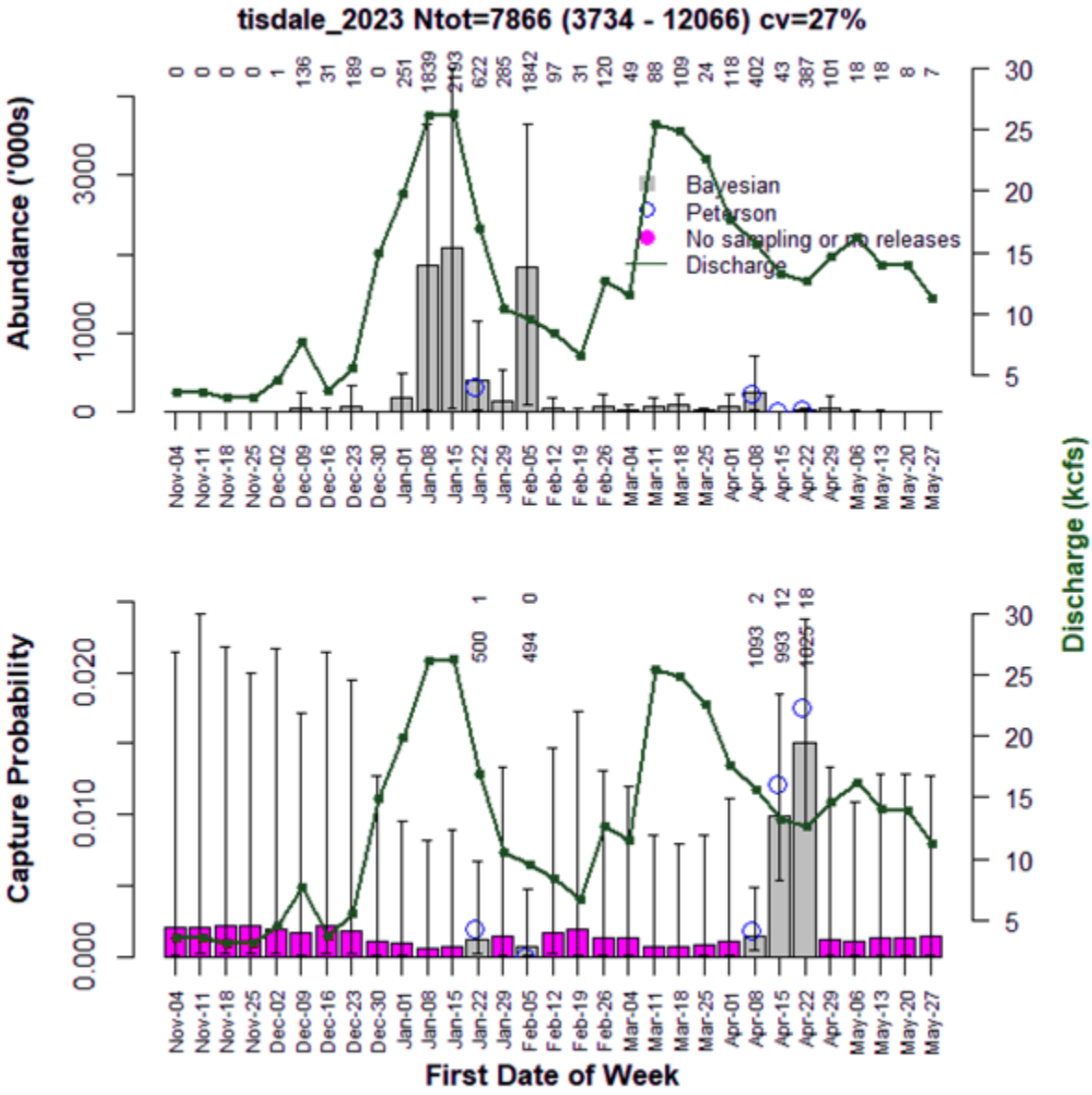

Figure 6. Time Series of Annual Abundance Estimates at Knights Landing and Tisdale Rotary Screw Trap Sites

Time series of annual abundance estimates for outmigrating juvenile Chinook salmon (all run types) at Knights Landing and Tisdale RST sites on the Sacramento River. The bar height and error bars represent the means and 95% credible intervals, respectively. The horizontal dashed line represents the mean across years.

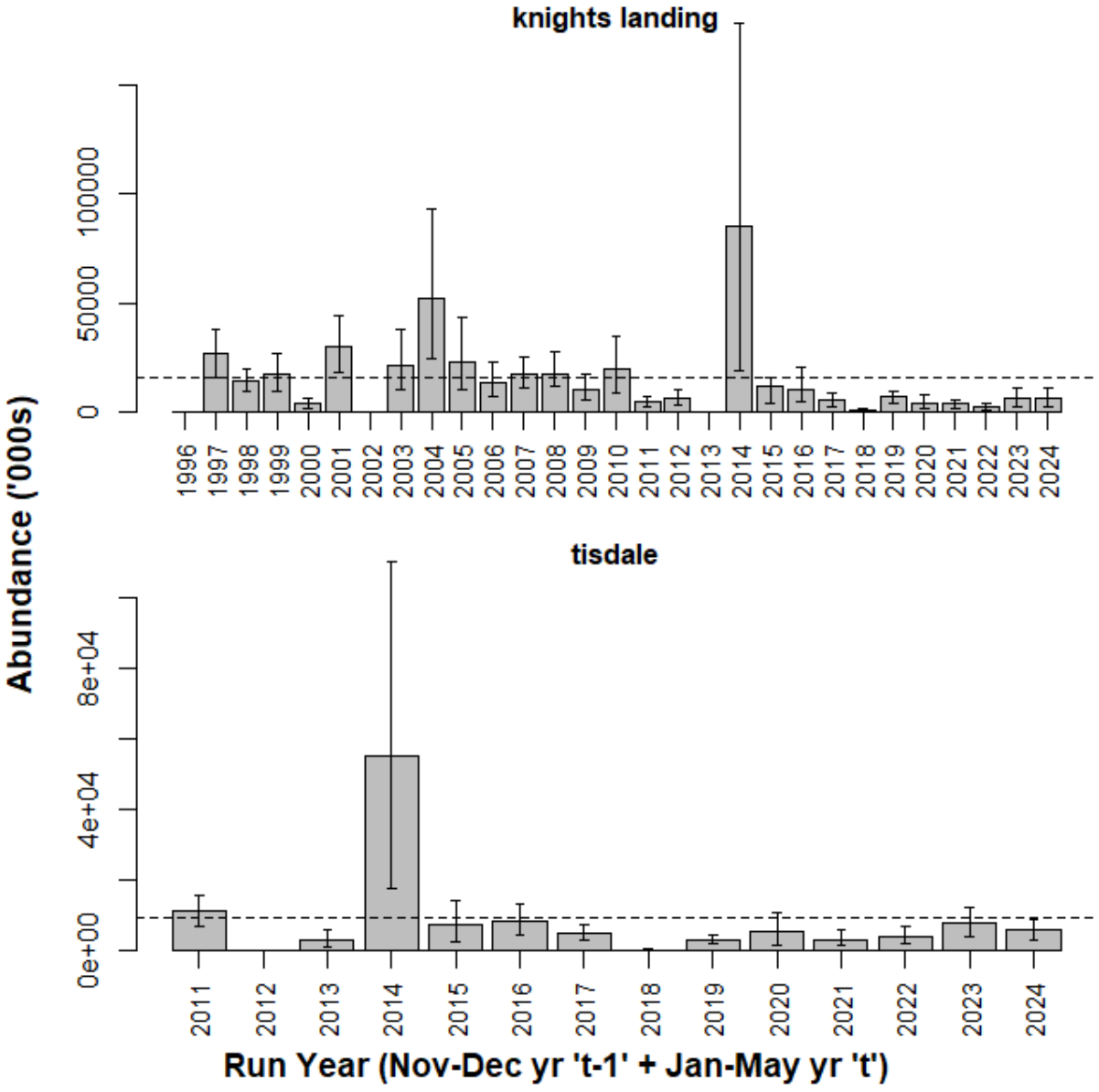

Figure 7. Run Year 2017 Predicted Weekly Abundance, Proportion of Spring-Run Chinook Salmon Estimated from Probabilistic Length-at-Date Model, and Estimated Abundance at Knights Landing Rotary Screw Trap Site

Predicted weekly abundance for juvenile outmigrating Chinook salmon (all run types, top panel), the proportion of spring-run estimated from the PLAD model (middle panel), and resulting estimated abundance of spring-run (bottom panel) at the Knights Landing RST site for run year 2017. The bar height and error bars represent median values and 95% credible intervals, respectively. The titles for the top and bottom panels show the median, 95% credible interval (in parentheses), and the CV of the annual outmigrant abundance estimates. Refer to Appendix B for the full set of results (27 run years for Knights Landing, 13 run years for Tisdale).

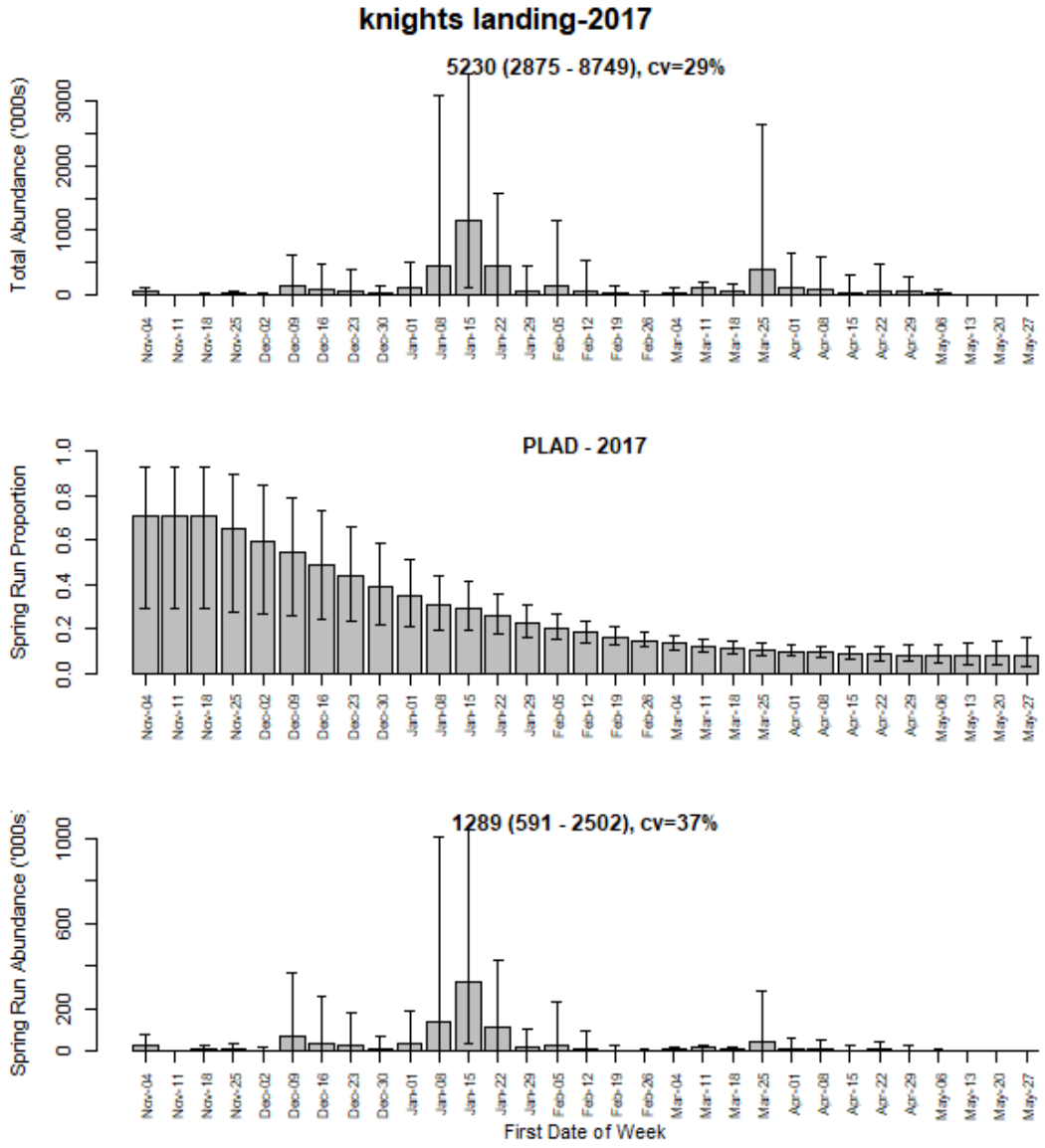

Figure 8. Time Series of Annual Outmigrant Abundance Estimates at Knights Landing and Tisdale Rotary Screw Trap Sites

Time series of annual (run year) juvenile outmigrant abundance estimates for spring-run at Knights Landing and Tisdale RST sites on the Sacramento River. The bar height and error bars represent the means and 95% credible intervals, respectively. The horizontal dashed line represents the mean across years.

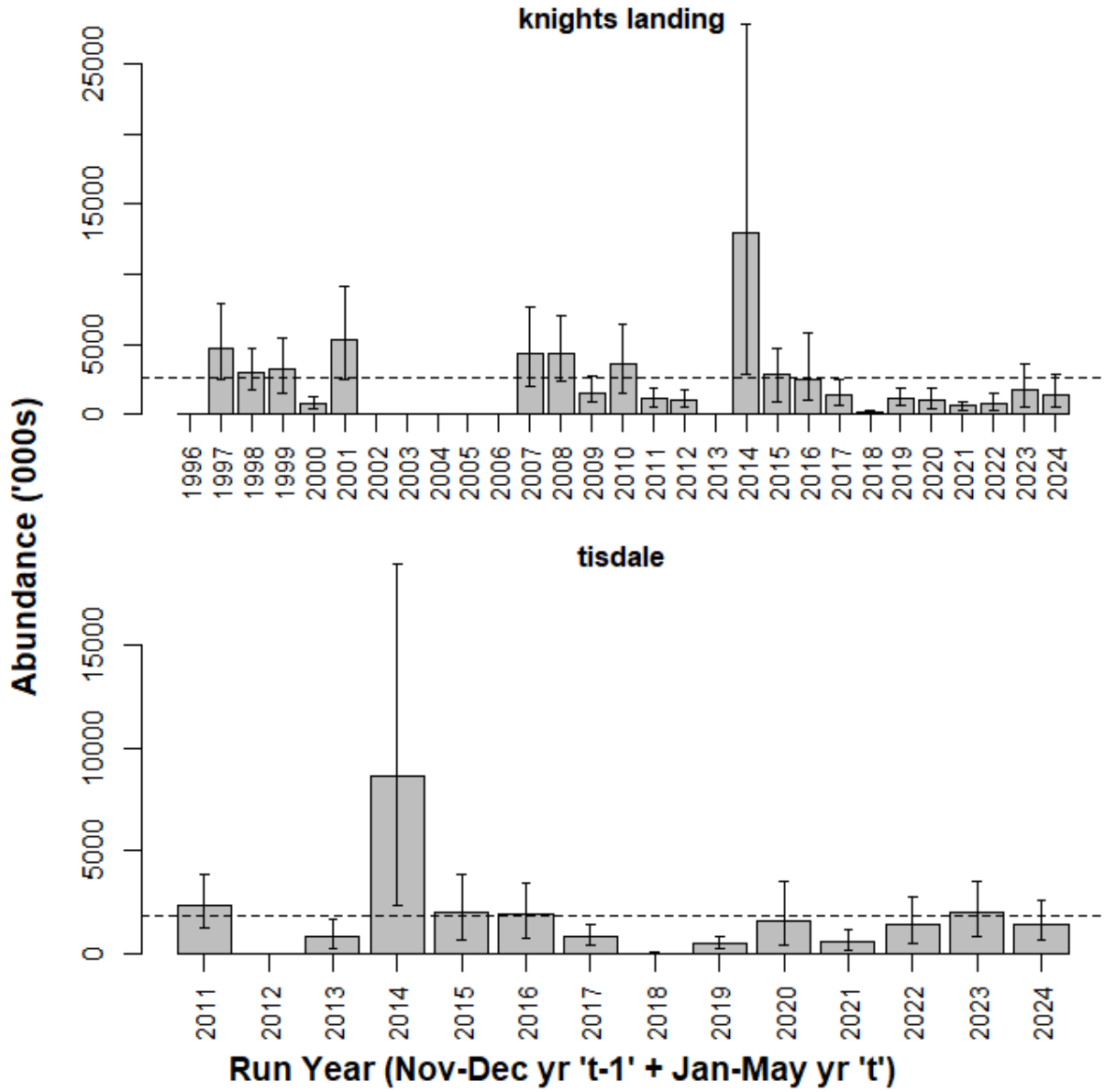

A. Predictions of Weekly Capture Probabilities of Chinook Salmon Abundances (All Runs)

Plots of weekly abundance of juvenile Chinook salmon outmigrants (all run types combined) and capture probability for all mainstem site years (main_all.pdf).

B. Predictions of Weekly Probabilistic Length-at-Date Predictions and Spring-run Abundances

Plots of weekly abundance of juvenile Chinook salmon outmigrants (all run types combined, top panels), PLAD predictions of the proportion of spring-run (middle panels), and resulting predictions of spring-run outmigrant abundance (lower panels, main_sr.pdf)